



## Solubility Studies of Sulfates of Copper, Zinc and Cobalt in Phosphoric Acid at 30 °C

DILBAR RAMAZONOVA<sup>1,✉</sup>, SHAVKAT UMAROV<sup>2,✉</sup>, AISHOLPAN SHAMISHOVA<sup>3,✉</sup>,  
KHILOLA MAMATOVA<sup>4,✉</sup>, NURBEK AYAKULOV<sup>4,✉</sup> and MURODJON SAMADIY<sup>1,\*✉</sup>

<sup>1</sup>Department of Chemical Technology of Inorganic Substances, Yangiyer branch of Tashkent Chemical Technological Institute, 1 Tinchlik str., Yangiyer, Uzbekistan

<sup>2</sup>Jizzakh Polytechnic Institute, 4 Islom Karimov st., 130100 Jizzakh, Uzbekistan

<sup>3</sup>Termez Institute of Agrotechnologies and Innovative Development, 288a I.Karimov st., 191200, Termez, Uzbekistan

<sup>4</sup>Gulistan State Pedagogical Institute, 4 Gulistan st., 120204 Gulistan, Uzbekistan

\*Corresponding author: Tel: +998 971380385, E-mail: samadiy@inbox.ru

Received: 14 August 2023;

Accepted: 24 August 2023;

Published online: 31 August 2023;

AJC-21376

Present study reports the isothermal experiments conducted at 30 °C to ascertain the solubility of copper, zinc and cobalt sulfates in phosphoric acid. The solubility diagram of  $\text{CuSO}_4\text{-H}_3\text{PO}_4\text{-H}_2\text{O}$  system is shown to have one branch, this is equivalent to the discharge of copper sulfate pentahydrate into the equilibrium solid phase. The solubility diagrams of zinc and cobalt sulfates have two branches of salt crystallization, corresponding to the release of hexahydrates and monohydrates of zinc and cobalt with increasing phosphoric acid content, saturated solutions in the  $\text{ZnSO}_4\text{-H}_3\text{PO}_4\text{-H}_2\text{O}$  and  $\text{CoSO}_4\text{-H}_3\text{PO}_4\text{-H}_2\text{O}$  systems become more viscous and denser, reaching a maximum at the transition point, while these indicators in the  $\text{CuSO}_4\text{-H}_3\text{PO}_4\text{-H}_2\text{O}$  system only increase.

**Keywords:** Sulfates of copper, Zinc, Cobalt, Phosphoric acid, Isothermal.

### INTRODUCTION

For normal growth and development of plants, various nutrients are needed. Based on contemporary data, it has been shown that around 70 elements are essential for plants to successfully undergo their developmental cycle and these elements are irreplaceable by alternative substances [1,2]. Copper sulfate pentahydrate is widely recognized as the foremost industrial copper compound, with diverse applications encompassing fungicides, soil additives and the manufacturing of copper compounds in bulk for commercial purposes [3].

In addition to the main macronutrients, namely nitrogen, phosphorous, potassium, calcium, magnesium and sulfur, microelements are also essential for the optimal growth and development of plants. The essential significance of fourteen trace elements has been firmly established. These include copper, zinc, cobalt, nickel, manganese, molybdenum, boron, *etc.*, which part of enzymes, vitamins, hormones, segments and other compounds that affect life processes. An increase in the application rates of the main nutrients-nitrogen, phosphorus and potassium has practically no effect on increasing the yield [4], in particular,

of cotton [5,6]. The global demand for microelements containing fertilizers is on the rise, leading to an expansion in their production and consumption worldwide [7]. Trace elements are commonly employed in traditional agricultural practices, specifically through pre-sowing treatment of seeds and foliar feeding of plants at different stages of their growth [8,9].

There is an established data, which supports the claim that microelement use in agriculture is highly effective. More and more attention is being paid to the issue of making and using fertilizers with trace elements. Many variables, including the widespread adoption of innovative farming practices including rock irrigation, hydromomics and foliar feeding of plants, are responsible for this uptick in quality and output [10]. One of the most promising, agrochemicals and economically viable ways of using microelements is their introduction into the composition of mineral fertilizers [11-13]. At the same time, the quality indicators of raw cotton are improved and productivity is increased. The costs associated with their production, transportation, storage, and use are minimized and a uniform distribution of micro-components across the entire sown area is achieved. Henceforth, this work has focused on incorporating the sulfate salts of

trace elements like copper, zinc and cobalt into the phosphoric acid to create phosphate fertilizers with these nutrients. In order to achieve the intended objective, a comprehensive investigation was conducted on various systems, which comprises copper sulfate, cobalt sulfate, zinc sulfate and phosphoric acid at 30 °C.

### EXPERIMENTAL

In order to conduct an analysis of the mineral composition of zinc, a quantity of 200 mg of suspension was measured using an analytical balance (FA220 4N). The mineralization process was performed using a mineralization machine (MILESTONE Ethos Easy, Italy). In test tube, 200 mg of sample, 2 mL of H<sub>2</sub>O<sub>2</sub> and 6 mL of HNO<sub>3</sub> were thoroughly mixed, which acted as an oxidizing agent and the whole mixture underwent mineralization within 40 min. After the mineralization process, the solution was subsequently transferred into an Erlenmeyer flask and diluted with 40 mL of distilled water.

Finally, the flask with the sample mixture was transferred to a separate tube in a automation section and analyzed using inductively coupled techniques. Determination of Zn was performed by using the X-ray fluorescence analysis method [14,15]. This approach can be repeated with high precision and minimal impact on the environment in order to ascertain the Zn concentration.

Solid phases were identified by chemical, X-ray phase, IR spectroscopic, X-ray fluorescence, atomic absorption and microscopic methods of analysis. All the X-ray samples were processed on Jindao XRD-6100, which can perform X-ray intensity analysis, crystallization analysis, stress analysis and retained austenite analysis. The utilization of the diffractometer XRD-6100, in conjunction with the vertical goniometer theta-2θ, has been designated as the primary approach for resolving a the peaks in the studied systems.

### RESULTS AND DISCUSSION

At 30 °C, copper sulfate-phosphoric acid-water system was investigated using the isothermal solubility method. The first phase of crystallization in the system's solubility diagram at 30 °C represents the release of copper sulfate pentahydrate into the equilibrium solid phase (Fig. 1). The solubility of copper sulfate reduces from 20 wt.% to 7.77 wt.% when phosphoric acid was introduced to the saturated solutions (Table-1). How-

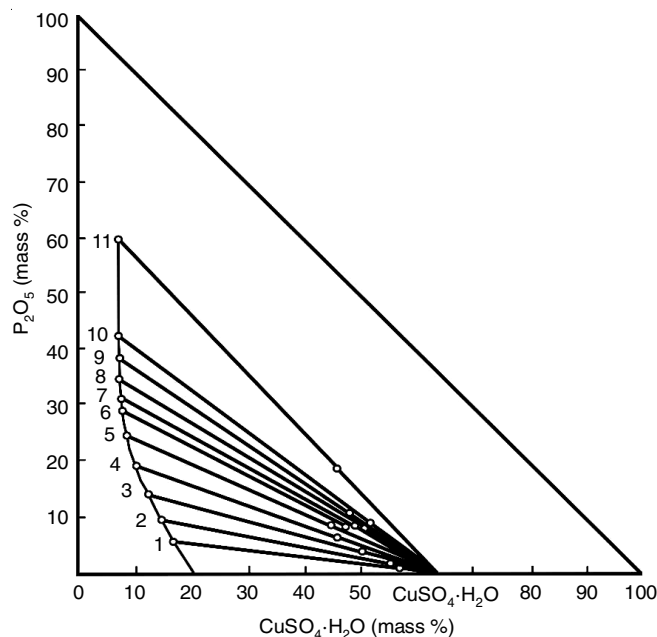


Fig. 1. Solubility isotherm of CuSO<sub>4</sub>-H<sub>3</sub>PO<sub>4</sub>-H<sub>2</sub>O system at 30 °C

ever, the solubility of copper sulfate does not change even when the concentration of phosphoric acid is increased to 31.40% or higher in terms of phosphoric anhydride.

The saturated solutions of copper sulfate, phosphoric acid, and water at 30 °C show that the density (Fig. 2a) and viscosity (Fig. 2b) of these solutions increase with increasing phosphoric acid content. The first curve in the graph depicts the process of crystallization of zinc sulfate hexahydrate, while the second branch corresponds to the introduction of zinc sulfate monohydrate into the solid phase. The conversion of zinc sulfate hexahydrate to zinc sulfate monohydrate occurs upon the addition of phosphoric acid to a saturated solution of zinc sulfate in its solid state (Table-2). The solubility of zinc sulfate reduces as the concentration of phosphoric acid increases. The conversion of zinc sulfate from hexahydrate to monohydrate occurs when the ratio of ZnSO<sub>4</sub>:P<sub>2</sub>O<sub>5</sub> was 22.39%:26.60% [16].

Moreover, in ZnSO<sub>4</sub>-H<sub>3</sub>PO<sub>4</sub>-H<sub>2</sub>O and the CoSO<sub>4</sub>-H<sub>3</sub>PO<sub>4</sub>-H<sub>2</sub>O ternary systems also have two curves of crystallization on their isotherms at 30 °C (Fig. 3). The cobalt sulfate hexahydrate was released into the solid phase along the first curve and the cobalt sulfate monohydrate crystallization is repres-

TABLE-1  
SOLUBILITY DATA OF CuSO<sub>4</sub>-H<sub>3</sub>PO<sub>4</sub>-H<sub>2</sub>O SYSTEM AT 30 °C

Composition points	Liquid phase's composition (wt.%)		Solid's "residue" composition (wt.%)		ρ (g/cm <sup>3</sup> )	μ (cSt)	Solid phase
	P <sub>2</sub> O <sub>5</sub>	CuSO <sub>4</sub>	P <sub>2</sub> O <sub>5</sub>	CuSO <sub>4</sub>			
1	5.61	16.87	0.75	57.24	1.2704	–	CuSO <sub>4</sub> ·5H <sub>2</sub> O
2	9.55	14.60	1.32	55.39	1.2837	–	CuSO <sub>4</sub> ·5H <sub>2</sub> O
3	14.29	12.36	3.62	50.42	1.3139	2.9790	CuSO <sub>4</sub> ·5H <sub>2</sub> O
4	18.51	10.53	6.35	46.03	–	–	CuSO <sub>4</sub> ·5H <sub>2</sub> O
5	24.40	8.89	8.22	44.85	1.3647	3.6840	CuSO <sub>4</sub> ·5H <sub>2</sub> O
6	28.92	8.18	8.38	47.84	1.4097	3.8910	CuSO <sub>4</sub> ·5H <sub>2</sub> O
7	31.40	7.79	8.12	49.20	1.4248	4.3571	CuSO <sub>4</sub> ·5H <sub>2</sub> O
8	34.70	7.77	7.75	51.00	1.4598	4.9108	CuSO <sub>4</sub> ·5H <sub>2</sub> O
9	37.99	7.77	10.09	48.53	–	5.7003	CuSO <sub>4</sub> ·5H <sub>2</sub> O
10	42.60	7.77	9.07	52.18	1.5598	8.0986	CuSO <sub>4</sub> ·5H <sub>2</sub> O
11	60.05	7.77	18.51	46.50	–	–	CuSO <sub>4</sub> ·5H <sub>2</sub> O

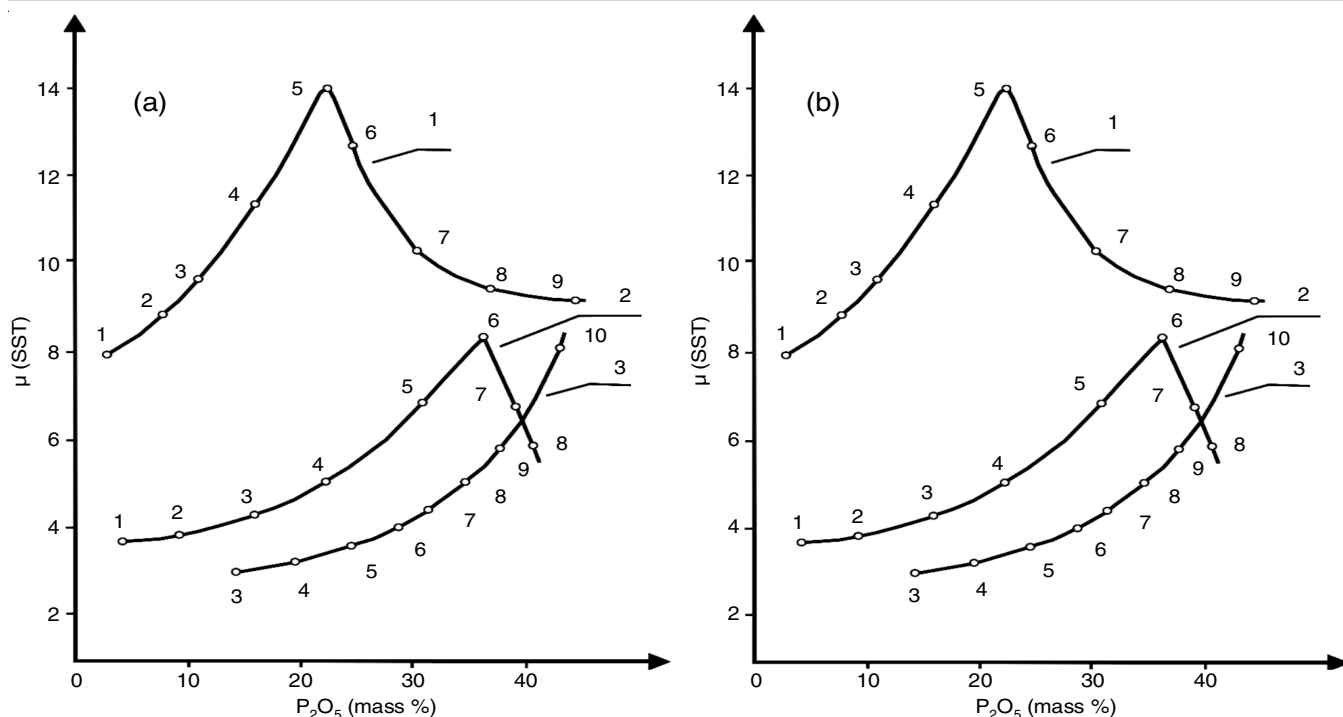


Fig. 2. Change in (a) viscosity and (b) density of the saturated solutions in the  $\text{ZnSO}_4\text{-H}_3\text{PO}_4\text{-H}_2\text{O}$  (1),  $\text{CoSO}_4\text{-H}_3\text{PO}_4\text{-H}_2\text{O}$  (2) and  $\text{CuSO}_4\text{-H}_3\text{PO}_4\text{-H}_2\text{O}$  (3) systems at 30 °C

TABLE-2  
SOLUBILITY DATA OF  $\text{ZnSO}_4\text{-H}_3\text{PO}_4\text{-H}_2\text{O}$  SYSTEM AT 30 °C

Composition points	Liquid phase's composition (wt.%)		Solid's "residue" composition (wt.%)		$\rho$ (g/cm <sup>3</sup> )	$\mu$ (cSt)	Solid phase
	P <sub>2</sub> O <sub>5</sub>	ZnSO <sub>4</sub>	P <sub>2</sub> O <sub>5</sub>	ZnSO <sub>4</sub>			
1	2.32	37.70	0.70	52.96	1.5335	7.969	ZnSO <sub>4</sub> ·6H <sub>2</sub> O
2	6.55	35.04	2.40	49.97	1.5496	–	ZnSO <sub>4</sub> ·6H <sub>2</sub> O
3	11.25	32.95	3.18	51.06	1.5678	9.739	ZnSO <sub>4</sub> ·6H <sub>2</sub> O
4	15.83	30.36	3.99	52.31	1.5865	11.359	ZnSO <sub>4</sub> ·6H <sub>2</sub> O
5	22.39	26.60	2.25	67.86	1.6211	13.778	ZnSO <sub>4</sub> ·6H <sub>2</sub> O + ZnSO <sub>4</sub> ·H <sub>2</sub> O
6	22.98	24.51	6.13	72.63	1.5900	–	ZnSO <sub>4</sub> ·H <sub>2</sub> O
7	25.07	22.04	6.13	74.09	1.5972	12.709	ZnSO <sub>4</sub> ·H <sub>2</sub> O
8	27.41	19.19	6.69	73.19	1.5812	–	ZnSO <sub>4</sub> ·H <sub>2</sub> O
9	30.57	17.05	6.68	73.53	1.5702	10.319	ZnSO <sub>4</sub> ·H <sub>2</sub> O
10	36.95	12.21	11.46	65.88	–	–	ZnSO <sub>4</sub> ·H <sub>2</sub> O
11	43.40	8.39	15.09	61.08	–	9.134	ZnSO <sub>4</sub> ·H <sub>2</sub> O
12	54.40	4.67	17.59	62.07	–	–	ZnSO <sub>4</sub> ·H <sub>2</sub> O
13	59.40	3.44	17.86	63.63	–	–	ZnSO <sub>4</sub> ·H <sub>2</sub> O

TABLE-3  
SOLUBILITY DATA OF  $\text{CoSO}_4\text{-H}_3\text{PO}_4\text{-H}_2\text{O}$  SYSTEM AT 30 °C

Composition points	Liquid phase's composition (wt.%)		Solid's "residue" composition (wt.%)		D (g/cm <sup>3</sup> )	$\mu$ (cSt)	Solid phase
	P <sub>2</sub> O <sub>5</sub>	CoSO <sub>4</sub>	P <sub>2</sub> O <sub>5</sub>	CoSO <sub>4</sub>			
1	3.71	24.98	0.63	52.50	1.3 693	3.6733	CoSO <sub>4</sub> ·6H <sub>2</sub> O
2	9.38	22.44	2.79	49.67	1.3705	3.9785	CoSO <sub>4</sub> ·6H <sub>2</sub> O
3	15.62	18.85	3.95	48.63	1.3867	4.2481	CoSO <sub>4</sub> ·6H <sub>2</sub> O
4	22.14	15.49	6.03	47.30	1.4213	4.9900	CoSO <sub>4</sub> ·6H <sub>2</sub> O
5	30.73	13.04	2.89	54.83	1.5618	6.7340	CoSO <sub>4</sub> ·6H <sub>2</sub> O
6	36.24	12.50	14.034	8.19	1.6886	8.3385	CoSO <sub>4</sub> ·6H <sub>2</sub> O + CoSO <sub>4</sub> ·H <sub>2</sub> O
7	38.63	8.85	10.04	67.48	1.6482	6.6923	CoSO <sub>4</sub> ·H <sub>2</sub> O
8	42.58	5.07	11.85	65.93	1.5908	5.1495	CoSO <sub>4</sub> ·H <sub>2</sub> O
9	46.69	3.27	15.60	60.62	–	–	CoSO <sub>4</sub> ·H <sub>2</sub> O
10	51.84	2.15	15.01	63.98	–	–	CoSO <sub>4</sub> ·H <sub>2</sub> O
11	63.82	2.13	19.45	62.57	–	–	CoSO <sub>4</sub> ·H <sub>2</sub> O

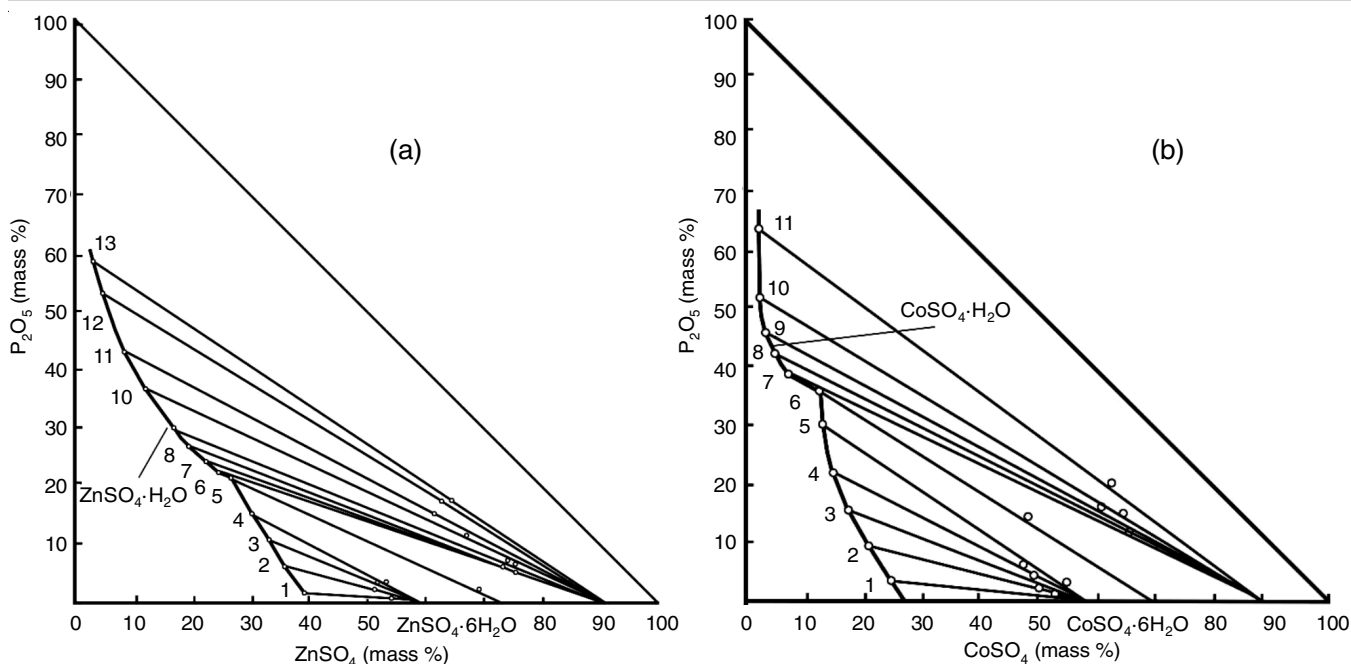


Fig. 3. Solubility isotherm of the (a)  $\text{ZnSO}_4\text{-H}_3\text{PO}_4\text{-H}_2\text{O}$  and (b)  $\text{CoSO}_4\text{-H}_3\text{PO}_4\text{-H}_2\text{O}$  system at 30 °C

ented by the second curve. The solubility of  $\text{CoSO}_4$  decreases as the concentration of phosphoric acid increases (Table-3). The equilibrium between  $\text{CoSO}_4\cdot 6\text{H}_2\text{O}$  with monohydrate and the liquid phase occurs at a specific point characterized by a composition of 36.24%  $\text{P}_2\text{O}_5$  and 12.50%  $\text{CoSO}_4$ .

The  $\text{CoSO}_4\text{-H}_3\text{PO}_4\text{-H}_2\text{O}$  system exhibits similar behavior to the  $\text{ZnSO}_4\text{-H}_3\text{PO}_4\text{-H}_2\text{O}$  ternary system, with changes in the viscosity and density of saturated solutions observed at 30 °C. These changes reach maximum peak at an acid concentration of 36.24% for phosphoric anhydride as shown in Fig. 2.

## Conclusion

The results obtained indicate the possibility of obtaining phosphorus-containing fertilizers by introducing copper sulphate, zinc sulphate and cobalt sulfate salts into the phosphoric acid. In this case, the isothermal solubility investigations conducted at 30 °C did not reveal any observable solubility patterns for phosphate solutions. However, it was observed that both zinc sulphate and cobalt sulphate underwent changes in their hydration states, while copper sulphate remained in its pentahydrate form.

## CONFLICT OF INTEREST

The authors declare that there is no conflict of interests regarding the publication of this article.

## REFERENCES

- Y. Ma, A. Xu and Z.M.M. Cheng, *Hortic. Plant J.*, **7**, 552 (2021); <https://doi.org/10.1016/j.hpj.2020.05.007>
- A. Vega, J.A. O'Brien and R.A. Gutiérrez, *Curr. Opin. Plant Biol.*, **52**, 155 (2019); <https://doi.org/10.1016/j.pbi.2019.10.001>
- F.J. Justel, M.E. Taboada and Y.P. Jimenez, *J. Mol. Liq.*, **249**, 702 (2018); <https://doi.org/10.1016/j.molliq.2017.11.083>
- M. Jalali and R. Fakhri, *J. Food Compos. Anal.*, **102**, 104049 (2021); <https://doi.org/10.1016/j.jfca.2021.104049>
- J. Wang, G. Du, J. Tian, C. Jiang, Y. Zhang and W. Zhang, *Agric. Water Manage.*, **255**, 106992 (2021); <https://doi.org/10.1016/j.agwat.2021.106992>
- Y. Zhang, Y. Zhang, G. Liu, S. Xu, J. Dai, W. Li, Z. Li, D. Zhang, C. Li and H. Dong, *Field Crops Res.*, **261**, 107989 (2021); <https://doi.org/10.1016/j.fcr.2020.107989>
- K. Mikula, G. Izydorczyk, D. Skrzypczak, M. Mironiuk, K. Moustakas, A. Wittek-Krowiak and K. Chojnacka, *Sci. Total Environ.*, **712**, 136365 (2020); <https://doi.org/10.1016/j.scitotenv.2019.136365>
- L.C. Nunes, E.R. Pereira-Filho, M.B.B. Guerra and F.J. Krug, *Spectrochim. Acta B: Atom. Spectrosc.*, **64**, 565 (2019); <https://doi.org/10.1016/j.sab.2009.05.002>
- R. Moreno-Salazar, I. Sánchez-García, W. Chan-Cupul, E. Ruiz-Sánchez, H.A. Hernández-Ortega, J. Pineda-Lucatero and D. Figueroa-Chávez, *Sci. Hortic.*, **261**, 108950 (2020); <https://doi.org/10.1016/j.scienta.2019.108950>
- M. Sihlahla, H. Mouri, P.N. Nomngongo and *J. African Earth Sci.*, **160**, 103635 (2019); <https://doi.org/10.1016/j.jafrearsci.2019.103635>
- O.A. Osinuga, A.B. Aduloju and C.O. Oyegoke, *J. Trace Elem. Miner.*, **5**, 100090 (2023); <https://doi.org/10.1016/j.jtemin.2023.100090>
- X. Wang, J. Shen and H. Liao, *Plant Sci.*, **179**, 302 (2010); <https://doi.org/10.1016/j.plantsci.2010.06.007>
- P.S. Bindraban, C. Dimkpa, L. Nagarajan, A. Roy and R. Rabbinge, *Biol. Fert. Soils*, **51**, 897 (2015); <https://doi.org/10.1007/s00374-015-1039-7>
- A.G. Revenko, X-Ray Spectral Fluorescence Analysis of Natural Materials, Novosibirsk: Nauka, pp. 1-264 (1994).
- L.N. Mazalov, X-ray Spectra and Chemical Bond, Novosibirsk: Nauka, p. 111 (1982).
- T. Stanimirova, T. Kerestedian and G. Kirov, *Appl. Clay Sci.*, **135**, 16 (2017); <https://doi.org/10.1016/j.clay.2016.08.032>